Effect of Carbazolyl Groups on Photophysical Properties of Cyanuric Chloride

Weichen Gao,[†] Yan Su,[†] Zhonghao Wang,[†] Yongfeng Zhang,[†] Dan Zhang,[†] Peng Jia,[†] Chaolong Yang,*[,†,‡] Youbing Li,[†] Rakesh Ganguly,[‡] Yanli Zhao*[,‡]

[†]School of Materials Science and Engineering, Chongqing University of Technology, Chongqing 400054, PR China

[‡]Division of Chemistry and Biological Chemistry, School of Physical and Mathematical Sciences, Nanyang Technological University, 21 Nanyang Link, Singapore 637371

ABSTRACT: Long-lived room temperature organic phosphorescence is highly useful in biological imaging, electroluminescent devices, information security, and security protection on account of its unique photophysical process and long-lived luminescence. In recent years, pure organic phosphorescent materials that do not contain rare precious metals have received increasing attention. Carbazole and its derivatives have been used to develop room temperature organic phosphorescent materials. However, the effect of carbazolyl groups on the photophysical properties of pure organic phosphors has rarely been reported. In this work, three cyanuric chloride phosphors (CzDCIT, BiCzDT and TCzT) modified with different numbers of carbazolyl groups were synthesized. Several characterization techniques were employed to reveal distinct crystal forms of CzDCIT, BiCzDT and TCzT. The single crystal diffraction of CzDCIT and BiCzDT showed not only different crystal packing modes, but also the formation of internal *H*-aggregation. These three phosphor powders exhibited dual emissions of blue fluorescence and yellow phosphorescence at room temperature, with luminescence lifetimes of 0.16-0.34s. Theoretical calculations indicated that different numbers of effective intersystem crossing channels between CzDCIT, BiCzDT or TCzT were responsible for the luminescence lifetimes. After doping the phosphors into the polymer matrix, they exhibited good persistent phosphorescence and high recoverability in multiple compression-grinding cycles.

KEYWORDS: carbazolyl group; cyanuric chloride; organic persistent luminescence; photophysical properties; polymer matrix; room temperature organic phosphorescence

■ INTRODUCTION

Organic materials that exhibit long-lived room temperature phosphorescence (RTP) present many fascinating applications such as in bioimaging,[1] electroluminescent devices,[2] information security,[3] organic light-emitting diodes,[4] photodynamic therapy,[5] anti-counterfeiting,[6,7] and molecular switches.[8] Conventional organic phosphorescent materials are usually coordination complexes containing precious metals.[9,10] The presence of precious metals enhances spin-orbit coupling, resulting in effective RTP. However, precious metals are expensive and also biologically toxic.[11] Thus, pure organic RTP materials without precious metals have gained more and more attention on account of their low cost, good processability, high stability and good biocompatibility.[12] So far, different strategies have been proposed to achieve pure organic RTP, including low temperature treatment,[13] heavy atom effects,[14] doping into polymer matrix,[15] integrating with steroidal compounds,[16] macrocycle encapsulation,[17] deuterium substitution,[18] host-guest doping,[19] forming organic frameworks,[20,21] *H*-aggregation,[22] crystalline inducement,[23] ionic crystals,[24] UV irradiation,[25] and using carbon dots.[26]

As far as the system itself is concerned, carbazole and its derivatives are widely used in the synthesis and development of pure organic phosphorescent materials. For example, Yang and co-workers combined heavy halogen atoms with carbazolyl group as the π unit to enhance the spin-orbit coupling and improve the intersystem crossing (ISC) rate. Based on this approach, orange RTP emission with the luminescence lifetime of up to 0.49s was observed.[27] Based on the chemical composition and molecular packing, An and co-workers reported that 4,6-diphenyl-2-carbazolyl-1,3,5-triazine (DPhCzT) could exhibit blue fluorescence and yellow phosphorescence having the phosphorescence lifetime of 1.06s. On one hand, the nitrogen atom in DPhCzT could promote n-π* transition, enhance spin-orbit coupling, and facilitate the ISC process. On the other hand, they found that obvious *H*-aggregation in the DPhCzT crystal is important means to effectively stabilize the excited triplet state. They then designed a series of organic compounds containing O, N and P atoms. By adjusting the structures, these organic compounds showed a change in the phosphorescence color from green to red under ambient conditions.[22]

Intelligent response materials with ultra-long organic phosphorescence (UOP) have been rarely reported. Gu and co-workers reported a chromophore consisting of carbazole and triazine units. By controlling the intermolecular interactions under UV light irradiation, the non-radiative transition of the excited triplet state was suppressed to emit ultra-long RTP. Based on dynamic UOP advantages, some phosphors could be used in intelligent response materials such as visual anti-counterfeiting.[28]

Compared with UV light, visible light has lower phototoxicity and is more readily available through cell phone flashlight and incandescent lamps. Therefore, UOP materials excited by visible light have great research value and application scope. To this end, Huang *et al.* synthesized aromatic amide derivatives with halogen substituents for achieving bright UOP under visible light excitation. The intermolecular interaction in the *xy* plane of the compounds could effectively adjust the red shift of the absorption spectrum, while the *H*-aggregation on the *z*-axis stabilizes the excited triplet state of the molecule.[29]

Persistent organic phosphors based on boron-cluster have also been reported. Yan and co-workers synthesized organic compounds by connecting σ-aromatic carbonyl cages to the carboboron-carbazole group. In these phosphors, the carboborane unit as the electron acceptor could easily induce the ISC process by intramolecular σ and π coupling. In addition, the rigid carboborane could also inhibit the thermal motion of molecules through a variety of intermolecular interactions, thus stabilizing the excited triplet state.[30]

According to these research results, it is obvious to conclude that the carbazole group plays an extremely important role for achieving ultra-long organic RTP on account of its unique photophysical properties. However, true effect of the carbazolyl group on the photophysical properties of organic RTP compounds has still not been well understood. In this work, we designed and prepared three cyanuric chloride phosphors (CzDCIT, BiCzDT and TCzT) modified with different numbers of carbazolyl groups in order to reveal the structure-property relationship controlled by the carbazolyl group.

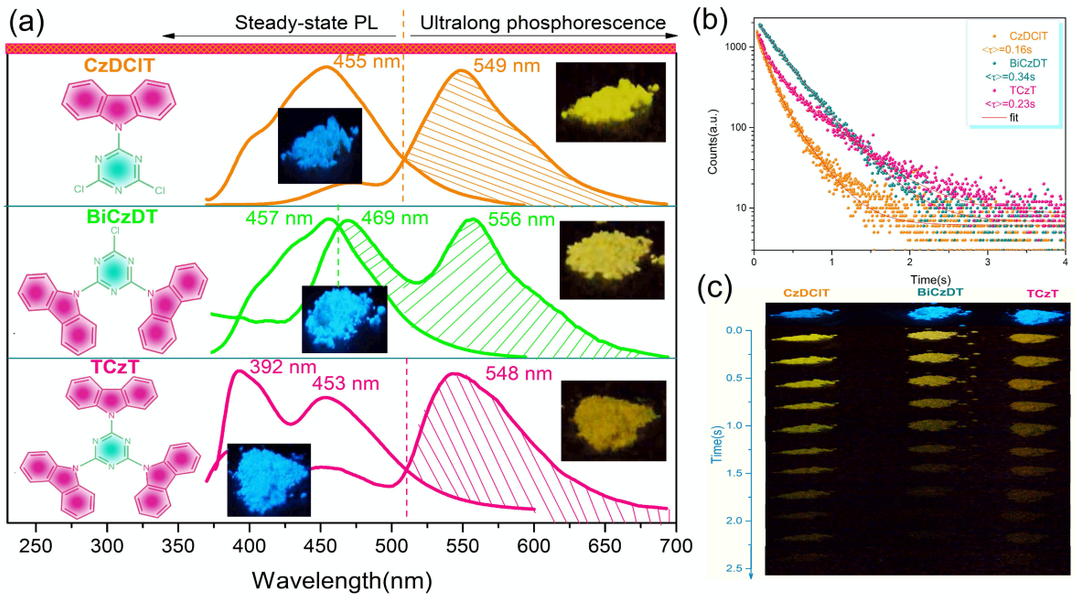

Figure 1. (a) Steady-state photoluminescence (PL) spectra (non-shadow) and ultralong phosphorescent spectra (shadow) of CzDCIT, BiCzDT, and TCzT powders. The spectra were recorded at room temperature upon 365 nm excitation and UV light removal. The insets show the corresponding molecular structures of the three phosphors and the photographs of the powders under two conditions. (b) Phosphorescence lifetime decay curves obtained at room temperature by recording the emission of CzDCIT powder at 549 nm, BiCzDT powder at 556nm, and TCzT powder at 548nm, under the excitation wavelength of 365nm. (c) Snapshots of CzDCIT, BiCzDT, and TCzT powders taken at different time intervals before (first row) and after (succeeding rows) turning-off the excitation (365 nm) under ambient conditions.

■ RESULTS AND DISCUSSION

In this work, cyanuric chloride, a widely used organic synthesis intermediate, and carbazole in different amounts were employed to synthesize three pure organic phosphors, *i.e.*, 9-(4,6-dichloro-1,3,5-triazin-2-yl)-9H-carbazol (CzDCIT), 9,9'-(6-chloro-1,3,5-triazine-2,4-diyl)bis(9H-c-arbazole) (BiCzDT), and 2,4,6-tri(9H-carbazol-9-yl)-1,3,5-triazine (TCzT) through a few simple steps (Figure S1 and Scheme S1). Nuclear magnetic resonance (NMR) spectroscopy, high-resolution mass spectrometry (HRMS), Fourier-transform infrared (FTIR) spectroscopy and thermogravimetric analysis confirmed their molecular structures (Figures S2-S9).

The effect of the carbazolyl group on organic photoluminescence properties was systematically investigated. As shown in Figure 1a, obvious blue fluorescence could be observed from all phosphor powders with the light excitation of 365 nm under ambient conditions. The fluorescence emission spectrum of CzDCIT shows an emission peak at 455 nm. Similarly, the emission peak of BiCzDT locates at 457 nm, and the emission peaks of TCzT are at 392 nm and 453 nm. Interestingly, after the removal of the UV light source, significant yellow long phosphorescence was observed from all powders. The RTP spectra and excitation-phosphorescence mapping show an maximum emission peak at 549 nm for CzDCIT, 469 nm and 556 nm for BiCzDT, and 548 nm for TCzT (Figures 1a and S10). The lifetime for the emission peaks of CzDCIT at 549 nm, BiCzDT at 556 nm, and TCzT at 548nm was measured to be 0.16s, 0.34s, and 0.23s respectively (Figure 1b), and corresponding phosphorescence quantum yields (Φ_P) were 1.14%, 1.45%, and 2.10% (Table S2), confirming their long RTP emission characteristics. At the same time, the entire process from fluorescence to long phosphorescence could be clearly observed by the naked eye or recorded by the camera (Figure 1c).

The excited triple state of organic compounds could be easily quenched by oxygen. In this work, however, similar steady-state photoluminescence spectra from all powders dispersed in tetrahydrofuran (THF) were measured in different conditions (nitrogen, vacuum, and ambient conditions), indicating the inactivity of the excited triplet states with oxygen (Figure S11). We also studied the effect of UV irradiation time on the photophysical properties of the three phosphors. The fluorescence emission intensity of all samples, whether in the powder state or dissolved in THF, was almost unchanged after exposure to 365 nm UV light for 100 min (Figure S12), indicating their high stability. More importantly, there was almost no change in the phosphorescence emission spectra of all powder samples. These robust characteristics broaden the application scope of these phosphors.

We then studied the temperature effect on photophysical properties of these three phosphors. At room temperature, only fluorescence emission was detected in THF solution for all phosphors, and no phosphorescence emission was observed due to molecular vibration in the solution. The fluorescence emission peaks for CzDCIT, BiCzDT, and TCzT were 474 nm, 467 nm, and 451 nm, and corresponding fluorescent lifetime was 1.57 ns, 1.25 ns, and 3.40 ns, respectively (Figure S13a,b). Upon changing temperature from room temperature to 77 K, the fluorescence emission peaks of all samples blue-shifted as compared with the ones at room temperature (Figure S13c). It could be inferred that the change of the fluorescence spectra with temperature is induced by the variation of molecular conformation. At the same time, CzDCIT, BiCzDT and TCzT showed more emission peaks in the fluorescence spectra at 77K, indicating that there were many non-radiative transition paths competing with the radiative transition paths of excited singlet states at room temperature. These non-radiative transition paths could be prohibited by low temperature such as at 77K.

Furthermore, it was more important to note that blue phosphorescence emission was observed in a glassy THF solution at 77K after turning off the UV lamp, and this continuous emission could last for up to 10s (Figure S14). At 77K, the phosphorescence emission peaks of CzDCIT, BiCzDT and TCzT center at 445, 451, and 449 nm respectively (Figure S13d), and they all show the phosphorescence lifetime in the range of 3.23s-3.45s (Table S2). As compared with the room temperature fluorescence emission spectra, the phosphorescence emission spectra of all samples at 77k also blue-shifted. These observations confirmed that molecular conformational hardening and rigid environment at low temperature could effectively suppress the non-radiative transition of the excited triplet states of molecules, leading to significant phosphorescence emission.

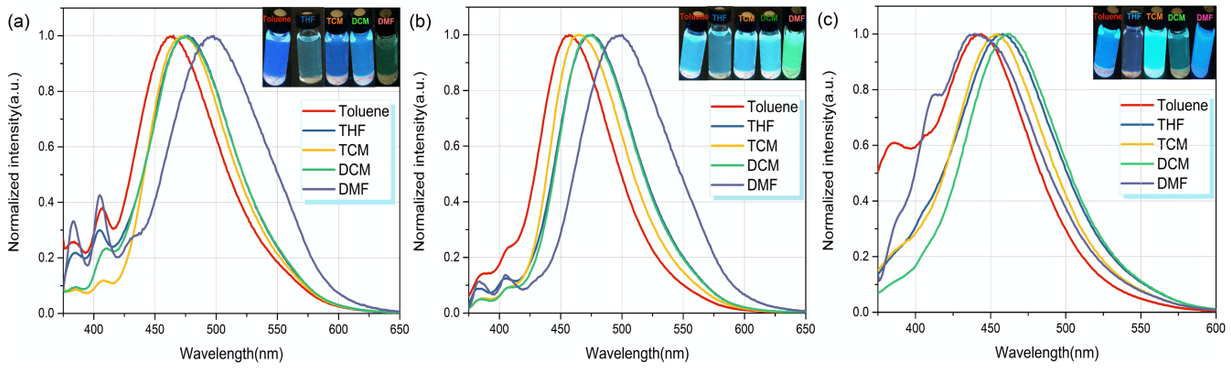

Figure 2. Fluorescence spectra of (a) CzDCIT, (b) BiCzDT, and (c) TCzT in toluene, THF, TCM, DCM, and DMF at room temperature. The insets show corresponding fluorescence colors in solution. The concentration was fixed at 1.0×10^{-5} M, and the excitation wavelength was 365 nm.

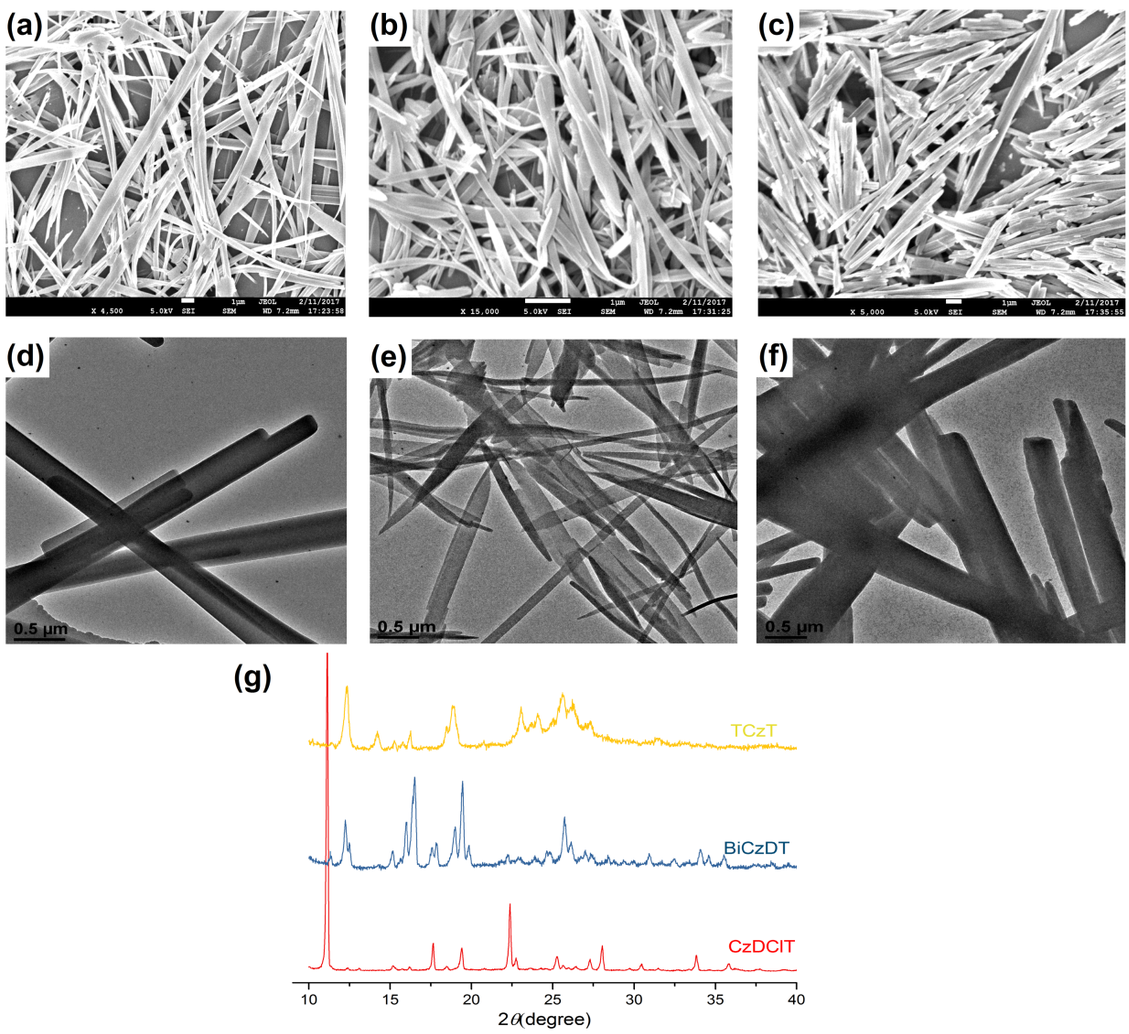

Figure 3. SEM images of (a) CzDCIT, (b) BiCzDT, and (c) TCzT aggregates. TEM images of (d) CzDCIT, (e) BiCzDT, and (f) TCzT aggregates. (g) Powder XRD patterns of CzDCIT, BiCzDT and TCzT. All molecular aggregates of CzDCIT, BiCzDT and TCzT were prepared in THF solution with a water content of 40 % at room temperature.

We then studied the photophysical properties of the three phosphors in organic solvents with different polarity. The organic solvents we selected are toluene, dichloromethane (DCM), THF, chloroform (TCM), and *N,N*-dimethylformamide (DMF), and corresponding polarity values are 2.4, 3.4, 4.2, 4.4, and 6.4. As the polarity of the solvent increases, slight red or blue shift of the absorption peaks could be observed in the UV-Vis absorption spectra of CzDCIT, BiCzDT, and TCzT (Figure S15). The fluorescence emission peaks of CzDCIT and BiCzDT were observed in the fluorescence spectra (Figure 2). Obvious red shifts of their fluorescence emission peaks of CzDCIT and BiCzDT were found upon increasing the solvent polarity. In particular, the fluorescence emission spectra of CzDCIT and BiCzDT in DMF with the strongest polarity showed the main emission peak at around 500 nm, giving green fluorescence emission. In other four organic solvents with weaker polarity, the main fluorescence emission peaks of CzDCIT and BiCzDT were approximately in the range of 460-475 nm, exhibiting blue fluorescence emission. Thus, the fluorescence emission peak in DMF red-shifted by about 40 nm as compared to the peak in toluene. For TCzT, however, the main fluorescence emission peaks were approximately in the range of 440-460 nm. Its fluorescence emission spectrum in DMF showed the main emission peak at around 440 nm and the shoulder peak at around 413 nm, presenting a significant blue shift as compared to those in DCM, TCM, and THF. The reason for the blue shift in DMF is probably due to that the interaction between TCzT and highly polar DMF solvent causes a change in the energy level between the ground state and the excited singlet state. Interestingly, the main peak positions in DMF and toluene were highly similar, all at around 440 nm. TCzT in these solvents exhibited significant blue emission.

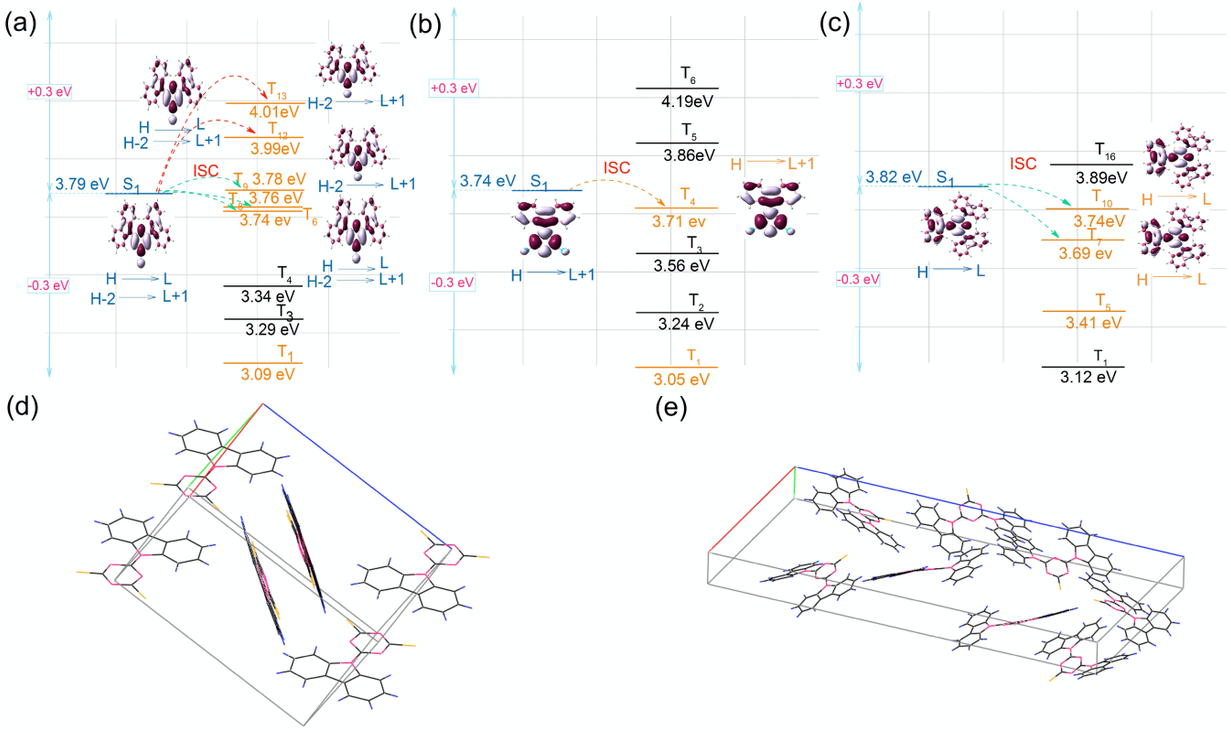

Figure 4. Schematic representation of the TDDFT calculation exhibiting the main orbital configurations, isosurface, and energy levels of (a) CzDCIT, (b) BiCzDT, and (c) TCzT in terms of monomer and co-planar dimer at the singlet (S_n) and triplet (T_n) states. L and H respectively indicate the lowest unoccupied molecular orbital and the highest occupied molecular orbital. Single crystal unit cells of (d) CzDCIT and (e) BiCzDT. These structures were drawn using Mercury program.

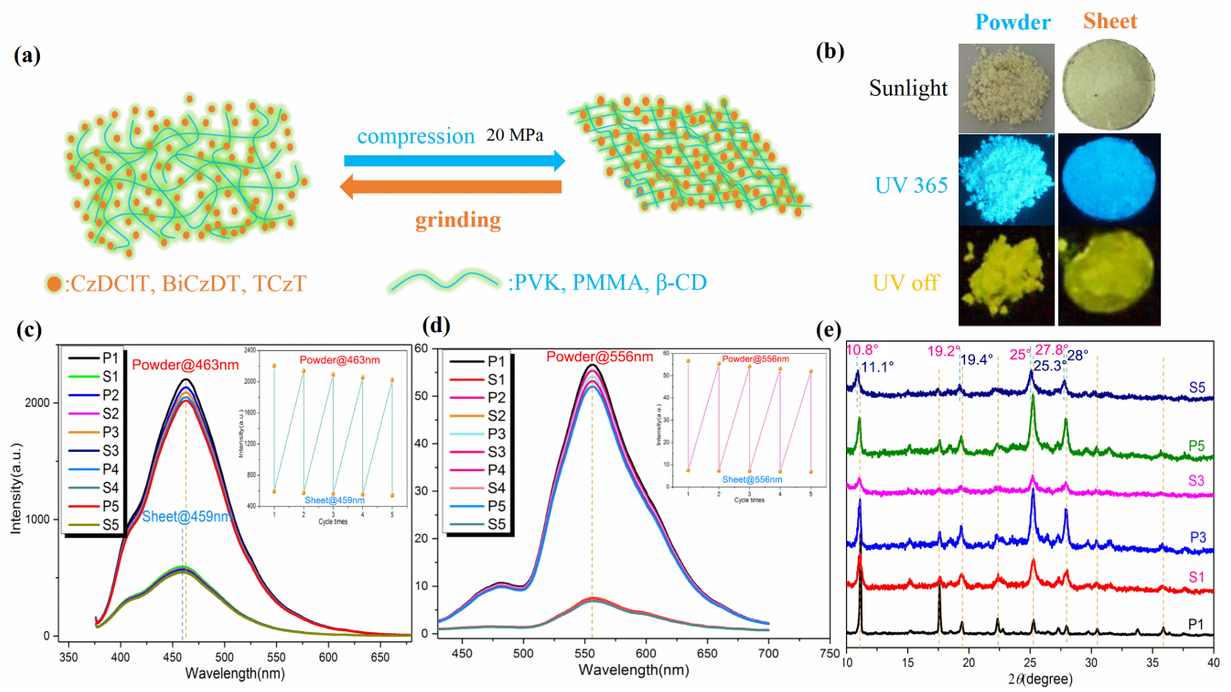

Figure 5. (a) Schematic compression (sheet) - grinding (powder) cycle of doped samples. (b) Photographs for powder and sheet samples of CzDCIT doped PMMA taken under different lighting conditions (sunlight, UV on, and UV off). (c) Fluorescence spectra of CzDCIT doped PMMA during five powder-sheet cycles. The inset shows corresponding powder and sheet fluorescence intensity during the five cycles. (d) Phosphorescence spectra of CzDCIT doped PMMA during five powder-sheet cycles. The inset shows corresponding powder and sheet phosphorescence intensity during the five cycles. (e) Powder XRD patterns of CzDCIT doped PMMA during five cycles. All the samples were treated upon the excitation at 365 nm.

To further understand the effect of the carbazolyl group on photophysical properties, the structural morphologies of the three phosphors were analyzed. Molecular aggregates formed in THF with a water content of 40% were studied by scanning electron microscope (SEM) and transmission electron microscope (TEM). As shown in Figure 3, the CzDCIT sample exhibited a long rod shape with a width of nearly one micrometer and a length of a few dozens of micrometers. The BiDCIT sample showed an elongated leaf shape with a width of several hundred nanometers and a length of several micrometers. For TCzT, the sample shape was short rod-like, with a width of several hundred nanometers and a length of only a few micrometers. Since the chemical structures of CzDCIT, BiCzDT and TCzT tend to be complex with the increase of carbazolyl groups, the crystallinity of the three phosphors decreases accordingly. Among them, CzDCIT exhibited the best crystallinity, with a large amount of high-quality crystals in the molecule. BiCzDT also showed a considerable number of good quality crystals, although its chemical structure is a bit more complicated than CzDCIT. For TCzT, on account of poor crystallinity caused by the complex chemical structure, it was impossible to obtain a large amount of high-quality crystals despite we tried many preparation methods. The crystallinity of CzDCIT, BiCzDT and TCzT samples was also studied by powder X-ray diffraction (XRD), and the difference in their crystallinity was further confirmed (Figure 3g).

In order to have further understanding on the mechanism of unique luminescence recorded from these three compounds, time-dependent density functional

theory (TDDFT) calculations on single molecules and assembled ones were carried out. As summarized in Figure 4a-c, when the triplet state energy level was above or below the first singlet state energy level at 0.3ev, singlet-triplet ISC process could occur. In addition, the isosurface and transition configurations of the excited singlet state (S_1) and excited triplet states were quite similar, thereby enhancing the spin-orbit coupling probability and thus the ISC process. For CzDCIT, only one channel ($S_1 \rightarrow T_4$) could participate in the effective ISC process. For BiCzDT, five channels ($S_1 \rightarrow T_6$, T_8, T_9, T_{12} and T_{13}) could be responsible for the effective ISC process. For TCzT, two channels ($S_1 \rightarrow T_7$ and T_{10}) would participate in the effective ISC process. On account of the increased number of energy transition channels, enhanced ISC process is supported, leading to the phosphor lifetime order of BiCzDT > TCzT > CzDCIT.

Furthermore, single crystal X-ray diffraction analysis was performed on CzDCIT and BiCzDT (Figure S16 and Table S1). The crystal structure of TCzT cannot be obtained on account of its poor crystallinity. In the crystal structures, as the carbazole unit increases, steric hindrance increases, resulting in twist angles between the planes of triazine unit and carbazole unit or between the planes of neighboring carbazole units, *i.e.*, these units are not co-planar. At the same time, this significant steric hindrance leads to different molecular packing modes in the crystal structures of CzDCIT and BiCzDT, as presented in Figures 4d,e and S17. In the dimer structures of CzDCIT and BiCzDT, the angle between the transition dipole and the interconnected axis (θ) is 86° and 77°, respectively. Both angles are greater than the critical value of 54.7°,[22] manifesting the presence of *H*-aggregation for effectively stabilizing the excited triplet state. As compared to CzDCIT, the distance between two molecules forming *H*-aggregation in BiCzDT increases, thus causing weakened *H*-aggregation (Figure S18). Furthermore, the *H*-aggregation formation was evidenced by a gradually blue-shifted absorption peak at 306 nm upon increasing the water content from 1% to 30% in methanol solutions of CzDCIT and BiCzD (Figure S19).

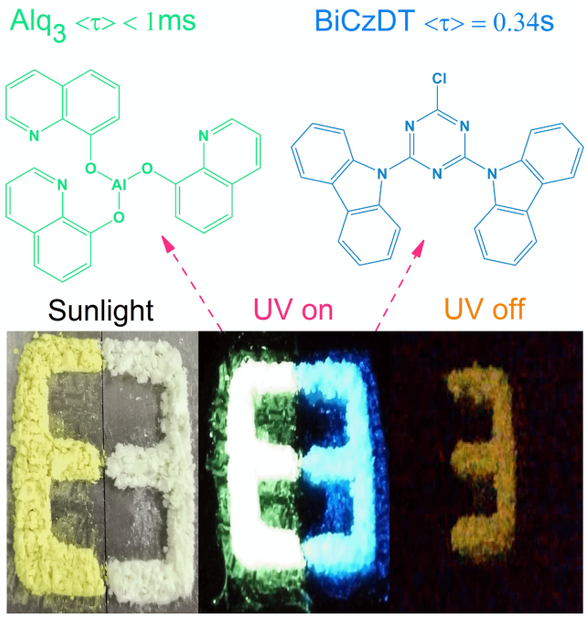

Figure 6. Photographs of pattern "8" taken under different lighting conditions (sunlight, UV on, and UV off). Pattern "8" consists of Alq_3 powder (left half) and BiCzDT powder (right half). Corresponding molecular structures of Alq_3 and BiCzDT are presented. UV excitation wavelength was 365 nm.

In order to better apply these phosphors, we doped these phosphors into different matrixes including polyvinyl carbazole (PVK), polymethylmethacrylate (PMMA), and β-cyclodextrin (β-CD), and studied their photophysical properties in detail. As shown in Figure S18, the phosphorescence emission curves of CzDCIT, BiCzDT and TCzT in the matrix were almost the same to those of corresponding undoped phosphors. Especially for CzDCIT, the contours of four phosphorescence emission curves almost overlapped by each other. After doping into the matrix, the phosphorescence intensity and lifetime of these phosphors did not change significantly, and all samples still exhibited good persistent phosphorescence properties.

Furthermore, we fabricated matrix sheets by applying a pressure of 20 MPa to the powder samples, and the results showed that these sheet samples were able to well maintain their persistent phosphorescent properties (Figures 5 and S20-S23). Taking CzDCIT doped PMMA as an example, both powders and sheets were milky white under sunlight, and no fluorescence or phosphorescence emission was observed (Figure 5). As expected, both powders and sheets samples emitted bright blue fluorescence under 365 nm UV irradiation, showing the same yellow phosphorescence after the UV lamp was turned off. Interestingly, the sample state could be switched between sheet and powder by compression and grinding. In order to quantitatively evaluate the photophysical property change of CzDCIT doped PMMA between the sheet and powder states, five sheet-powder cycles were measured. As shown in Figure 5c-e, after multiple compression and grinding cycles, the fluorescence and phosphorescence emission intensity of both sheet and powder samples could be restored to the initial status, exhibiting a high recoverability between the sheet and powder states. Powder XRD patterns of the sheet and powder samples further verified the good recoverability.

Surprisingly, above observation was contrary to the common decrease in fluorescence or phosphorescence intensity after grinding of the powder sample.[27,31,32] In our experiment, the fluorescence and phosphorescence intensity of the sheet sample was weaker than that of corresponding powder sample, and the position of the emission peak also showed an obvious shift. There were also shifts of the 2θ angles by 0.2° to 0.3° from their powder XRD patterns. The possible reason for the phenomena is that, after the CzDCIT doped PMMA powder is compressed, the contact distance between CzDCIT and PMMA matrix becomes closer, and at the same time, the contact area and degree between CzDCIT and PMMA matrix also increase. Macroscopically, non-luminous PMMA matrix provides a dilution effect to CzDCIT, resulting in a decrease in the CzDCIT concentration with decreased fluorescence and phosphorescence intensity.

On account of excellent persistent RTP properties of these phosphors, they are capable systems for data code applications. The digital pattern "8" presented in Figure 6 was composed of BiCzDT (right half) and 8-hydroxyquinoline aluminum (Alq_3, left half), a substance widely used as optoelectronic materials. Under the sunlight, the left and right sides of the pattern "8" showed light yellow and milky white, respectively. Under excitation with 365 nm UV lamp, the left and right sides were separated by bright green and blue fluorescence of Alq_3 and BiCzDT, respectively. After the UV lamp was turned off, only the right portion of the pattern "8" exhibited distinct yellow persistent phosphorescence contributed by BiCzDT. Thus, these phosphors with unique phosphorescence property showed highly promising application potential in data encryption and decryption.

■ CONCLUTIONS

In summary, we have designed three TRP phosphors in order to study the effect of the carbazolyl group on photophysical properties of cyanuric chloride derivatives. The results indicate that, although the three phosphors had similar fluorescence and phosphorescence dual-mode emission under ambient conditions, the

substitution number of the carbazolyl group presented a significant effect on their phosphorescence lifetime, fluorescence emission in different polar organic solvents, crystallization property, intramolecular ISC channels, and crystal stacking modes. In addition, phosphors doped into the matrix have also exhibited good persistent phosphorescence properties and recoverability in multiple powder-sheet cycles. As a proof of concept, the phosphors have been successfully employed for simple data code applications. Thus, the present research concerning the effect of the carbazolyl group on photophysical properties of pure organic phosphors serves as a useful reference for further design of advanced organic RTP materials.

■ EXPERIMENTAL SECTION

Synthesis of 9-(4,6-dichloro-1,3,5-triazin-2-yl)-9H-carbazol (CzDCIT). Carbazole (5.68 g) was added to a three-necked flask followed by adding dry THF (150 mL), which was completely dissolved and protected by N_2 for 10 min. *n*-BuLi (12.9 mL, 2 m) was gradually added by a dropping funnel, and the addition was completed in about 10 min. The reaction was carried out at 0 ℃. After the addition of *n*-BuLi, the reaction was continued at 0 ℃ for 30 min, and then degassed cyanuric chloride (4.86 g) and THF (120 mL) were added. The reaction was continued at 0 ℃ for 30 min. After reacting at room temperature for 30 min, the temperature was raised to 80 ℃ to reflux for 6 h. After the completion of the reaction, THF was removed by rotary evaporation, and the residue was washed with a large amount of acetone for 3-5 times to obtain CzDCIT (6.2g, yield: 59%) as a light-yellow powder. ^{1}H NMR (400Hz, $CDCl_3$): δ 8.85 (d, 2H), 7.98 (d, 2H), 7.51 (d, 2H), 7.45 (d, 2H). HRMS: 315.08 (M^{+1}), calculated for $C_{15}H_8N_4Cl_2$: 314.01.

Synthesis of 9,9'-(6-chloro-1,3,5-triazine-2,4-diyl) bis(9H-carbazole) (BiCzDT). By following a similar synthetic procedure for CzDCIT, BiCzDT (2.3g, yield: 27%) was prepared as a light yellow-green powder. ^{1}H NMR (400Hz, $CDCl_3$): δ 7.51 (m, 12H), 8.06 (m, 6H), 8.90 (m, 6H). HRMS: 446.11 (M^{+1}), calculated for $C_{27}H_{16}N_5Cl$: 445.11.

Synthesis of 2,4,6-tri (9H-carbazol-9-yl)-1,3,5-triazine (TCzT). By following a similar synthetic procedure for CzDCIT, TCzT (6.2g, yield: 71%) was synthesized as a white powder. ^{1}H NMR (400Hz, $CDCl_3$): δ 7.45 (m, 12H), 8.14 (m, 6H), 9.01 (m, 6H). HRMS: 577.21 (M^{+1}), calculated for $C_{39}H_{24}N_6$: 576.21.

■ ASSOCIATED CONTENT

Supporting Information

The Supporting Information is available free of charge on the ACS Publications website.

Methods, characterizations, and property investigations including Scheme S1, Figures S1-S23, and Tables S1 and S2. CIF crystal data files of BiCzDT (CCDC 1938910) and CzDCIT (CCDC 1938909).

■ AUTHOR INFORMATION

Corresponding Author

*yclzjun@163.com

*zhaoyanli@ntu.edu.sg

■ ACKNOWLEDGMENT

This work was financially supported by the National Natural Science Foundation of China (21875025), the special program of Chongqing Science and Technology Commission (cstc2018jcyjAX0296 and cstc2017zdcyzdyfX0007), Innovation Research Group at Institutions of Higher Education in Chongqing (CXQT19027), and the Science and Technology Research Program of Chongqing Municipal Education Commission (KJZD-K201801101 and KJ1709222). This research was also supported by the Singapore Agency for Science, Technology and Research (A*STAR) AME IRG grant (A1883c0005).

■ REFERENCES

(1) Zhen, X.; Tao, Y.; An, Z.; Chen, P.; Xu, C.; Chen, R.; Huang, W.; Pu, K. Ultralong Phosphorescence of Water - Soluble Organic Nanoparticles for *in Vivo* Afterglow Imaging. *Adv. Mater.* **2017,** *29*, 6665-6671.

(2) Hirata, S.; Totani, K.; Yamashita, T.; Adachi, C.; Vacha, M. Large Reverse Saturable Absorption under Weak Continuous Incoherent Light. *Nat. Mater.* **2014,** *13*, 938-946.

(3) Ying, L.; Ho, C. L.; Wu, H.; Cao, Y.; Wong, W. Y. White Polymer Light-Emitting Devices for Solid-State Lighting: Materials, Devices, and Recent Progress. *Adv. Mater.* **2014,** *26*, 2459-2473.

(4) Kabe, R.; Notsuka, N.; Yoshida, K.; Adachi, C. Afterglow Organic Light-Emitting Diode. *Adv. Mater.* **2016,** *28*, 655-660.

(5) Collins, H. A.; Khurana, M.; Moriyama, E. H.; Mariampillai, A.; Dahlstedt, E.; Balaz, M.; Kuimova, M.; Drobizhev, M.; Yang, V.; Phillips, D.; Rebane, A.; Wilson, B.; Anderson, H. Blood-Vessel Closure Using Photosensitizers Engineered for Two-Photon Excitation. *Nat. Photonics* **2008,** *2*, 420-424.

(6) Jiang, K.; Zhang, L.; Lu, J. F.; Xu, C. X.; Cai, C. Z.; Lin, H. W. Triple-Mode Emission of Carbon Dots: Applications for Advanced Anti-Counterfeiting. *Angew. Chem. Int. Ed.* **2016,** *55*, 7231-7235.

(7) Su, Y.; Zhang, Y.; Wang, Z.; Gao, W.; Jia, P.; Zhang, D.; Yang, C.; Li, Y.; Zhao, Y. Excitation-Dependent Long-Life Luminescent Polymeric Systems under Ambient Conditions. *Angew. Chem. Int. Ed.* **2019**, DOI: 10.1002/anie.201912102.

(8) Monaco, S.; Semeraro, M.; Tan, W. J.; Tian, H.; Ceroni, P.; Credi, A. Multifunctional Switching of a Photo- and Electro-Chemiluminescent Iridium–Dithienylethene Complex. *Chem. Commun.* **2012,** *48*, 8652-8654.

(9) van der Eeckhout, K.; Poelman, D.; Smet, P. F. Persistent Luminescence in Non-Eu^{2+}-Doped Compounds: A Review. *Materials* **2013,** *6*, 2789-2818.

(10) Xu, H.; Chen, R. F.; Lai, W. Y.; Su, Q. Q.; Huang, W.; Liu, X. G. Recent Progress in Metal-Organic Complexes for Optoelectronic Applications. *Chem. Soc. Rev.* **2014,** *43*, 3259-3302.

(11) Chen, H.; Yao, X. Y.; Ma, X.; Tian, H. Amorphous, Efficient, Room-Temperature Phosphorescent Metal-Free Polymers and Their Applications as Encryption Ink. *Adv. Opt. Mater.* **2016,** *4*, 1397-1401.

(12) Forni, A.; Lucenti, E.; Botta, C.; Cariati, E. Metal Free Room Temperature Phosphorescence from Molecular Self-Interactions in the Solid State. *J. Mater. Chem. C* **2018,** *6*, 4603-4626.

(13) Menning, S.; Krämer, M.; Coombs, B. A.; Rominger, F.; Beeby, A.; Dreuw, A.; Bunz, U. H. Twisted Tethered Tolanes: Unanticipated Long-Lived Phosphorescence at 77 K. *J. Am. Chem. Soc.* **2013,** *135*, 2160-2163.

(14) Xue, P. C.; Wang, P. P.; Chen, P.; Yao, B. Q.; Gong, P.; Sun, J. B.; Zhang, Z. Q.; Lu, R. Bright Persistent Luminescence from Pure Organic Molecules through a Moderate Intermolecular Heavy Atom Effect. *Chem. Sci.* **2017,** *8*, 6060-6065.

(15) Lee, D. W.; Bolton, O.; Kim, B. C.; Youk, J. H.; Takayama, S.; Kim, J. Room Temperature Phosphorescence of Metal-Free Organic Materials in Amorphous Polymer Matrices. *J. Am. Chem. Soc.* **2013,** *135*, 6325-6329.

(16) Katsurada, Y.; Hirata, S.; Totani, K.; Watanabe, T.; Vacha, M. Photoreversible On–Off Recording of Persistent Room-Temperature Phosphorescence. *Adv. Opt. Mater.* **2015,** *3,* 1726-1737.

(17) Chen, H.; Ma, X.; Wu, S. F.; Tian, H. A Rapidly Self-Healing Supramolecular Polymer Hydrogel with Photostimulated Room-Temperature Phosphorescence Responsiveness. *Angew. Chem. Int. Ed.* **2014,** *53*, 14149-14152.

(18) Hirata, S.; Totani, K.; Zhang, J. X.; Yamashita, T.; Kaji, H.; Marder, S. R.; Watanabe, T.; Adachi, C. Efficient Persistent Room Temperature Phosphorescence in Organic Amorphous Materials under Ambient Conditions. *Adv. Funct. Mater.* **2013,** *23*, 3386-3397.

(19) Xu, J. J.; Takai, A.; Kobayashi, Y.; Takeuchi, M. Phosphorescence from a Pure Organic Fluorene Derivative in Solution at Room Temperature. *Chem. Commun.* **2013,** *49,* 8447-8449.

(20) Yu, T.; Ou, D. P.; Yang, Z. Y.; Huang, Q. Y.; Mao, Z.; Chen, J. R.; Zhang, Y.; Liu, S. W.; Xu, J. R.; Bryce, M. R.; Chi, Z. G. The HOF Structures of Nitrotetraphenylethene Derivatives Provide New Insights into the Nature of AIE and a Way to Design Mechanoluminescent Materials. *Chem. Sci.* **2017,** *8,* 1163-1168.

(21) Xue, R.; Guo, H.; Wang, T.; Gong, L.; Wang, Y. N.; Ai, J. B.; Huang, D. D.; Chen, H. Q.; Yang, W. Fluorescence Properties and Analytical Applications of Covalent Organic Frameworks. *Anal. Methods* **2017**, *9*, 3737-3750.

(22) An, Z. F.; Zheng, C.; Tao, Y.; Chen, R. F.; Shi, H. F.; Chen, T.; Wang, Z. X.; Li, H. H.; Deng, R. R.; Liu, X. G.; Huang, W.

Stabilizing Triplet Excited States for Ultralong Organic Phosphorescence. *Nat. Mater.* **2015,** *14,* 685-690.
(23) Xie, Y. J.; Ge, Y. W.; Peng, Q.; Li, C. G.; Li, Q. Q.; Li, Z. How the Molecular Packing Affects the Room Temperature Phosphorescence in Pure Organic Compounds: Ingenious Molecular Design, Detailed Crystal Analysis, and Rational Theoretical Calculations. *Adv. Mater.* **2017,** *29*, 6829-6835.
(24) Cheng, Z. C.; Shi, H. F.; Ma, H. L.; Bian, L. F.; Wu, Q.; Gu, L.; Cai, S. Z.; Wang, X.; Xiong, W.-w.; An, Z. F.; Huang, W. Ultralong Phosphorescence from Organic Ionic Crystals under Ambient Conditions. *Angew. Chem. Int. Ed.* **2019,** *57*, 678-682.
(25) Su, Y.; Phua, S. Z.; Li, Y. B.; Zhou, X. J.; Jana, D.; Liu, G. F.; Lim, W. Q.; Ong, W. K.; Yang, C. L.; Zhao, Y. L. Ultralong Room Temperature Phosphorescence from Amorphous Organic Materials toward Confidential Information Encryption and Decryption. *Sci. Adv.* **2018,** *4,* eaas9732.
(26) Jiang, K.; Sun, S.; Zhang, L.; Lu, Y.; Wu, A. G.; Cai, C. Z.; Lin, H. W. Red, Green, and Blue Luminescence by Carbon Dots: Full-Color Emission Tuning and Multicolor Cellular Imaging. *Angew. Chem. Int. Ed.* **2015,** *54*, 5360-5363.
(27) Yang, Z. Y.; Mao, Z.; Zhang, X. P.; Ou, D. P.; Mu, Y. X.; Zhang, Y.; Zhao, C. Y.; Liu, S. W.; Chi, Z. G.; Xu, J. R.; Wu, Y. C.; Lu, P. Y.; Lien, A.; Bryce, M. Intermolecular Electronic Coupling of Organic Units for Efficient Persistent Room-Temperature Phosphorescence. *Angew. Chem. Int. Ed.* **2016,** *55*, 2181-2185.
(28) Gu, L.; Shi, H. F.; Gu, M. X.; Ling, K.; Ma, H. L.; Cai, S. Z.; Song, L. L.; Ma, C. Q.; Li, H.; Xing, G. C.; Hang, X. C.; Li, J. W.; Gao, Y. R.; Yao, W.; Shuai, Z. G.; An, Z. F.; Liu, X. G.; Huang, W. Dynamic Ultralong Organic Phosphorescence by Photoactivation. *Angew. Chem. Int. Ed.* **2018,** *57*, 8425-8431.
(29) Cai, S. Z.; Shi, H. F.; Li, J. W.; Gu, L.; Ni, Y.; Cheng, Z. C.; Wang, S.; Xiong, W.; Li, L.; An, Z. F.; Huang, W. Visible-Light-Excited Ultralong Organic Phosphorescence by Manipulating Intermolecular Interactions. *Adv. Mater.* **2017,** *29*, 1244-1249.
(30) Tu, D. S.; Cai, S. Z.; Fernandez, C.; Ma, H. L.; Wang, X.; Wang, H.; Ma, C. Q.; Yan, H.; Lu, C. S.; An, Z. F. Boron Cluster Enhanced Ultralong Organic Phosphorescence. *Angew. Chem. Int. Ed.* **2019,** *58*, 9129-9133.
(31) Gong, Y.; Chen, G.; Peng, Q.; Yuan, W. Z.; Xie, Y.; Li, S.; Zhang, Y.; Tang, B. Z. Achieving Persistent Room Temperature Phosphorescence and Remarkable Mechanochromism from Pure Organic Luminogens. *Adv. Mater.* **2015**, *27,* 6195–6201.
(32) Cai, S.; Shi, H.; Zhang, Z.; Wang, X.; Ma, H.; Gan, N.; Wu, Q.; Cheng, Z.; Ling, K.; Gu, M.; Ma, C.; Gu, L.; An, Z.; Huang, W. Hydrogen-Bonded Organic Aromatic Frameworks for Ultralong Phosphorescence by Intralayer π–π Interactions. *Angew. Chem. Int. Ed.* **2018**, *57*, 4005–4009.

Table of Contents Graphic